

## Supplementary Information

### **Hydrothermal treatment enhanced Z-scheme O-doped g-C<sub>3</sub>N<sub>4</sub>/WO<sub>3</sub> nanosheet for visible-light photocatalytic degradation of TC under different dissolved oxygen concentration**

Xiuling Xue<sup>1\*</sup>, Xiaoyi Chen<sup>1</sup>, Zongyu Zhang<sup>1</sup>.

College of Chemical Engineering, Huaqiao University, Xiamen, 361021, China

\* Corresponding Author: Xiuling Xue

E-mail: xueling@hqu.edu.cn

Telephone: +86-592-6162300

Fax: +86-5926162300

## Section 1. Experimental details

### Materials

The chemicals used in this study were of analytical grade. TC, BPA and CIP were supplied by Aladdin Reagent CO., Ltd. Melamine were purchased from Shanghai Macklin Biochemical Co., Ltd. Other chemicals were from Sinopharm Chemical Reagent Co., Ltd. Deionized (DI) water was used throughout this study which was produced by Milli-Q system.

### Recycle experiments

The stability and reusability of the OCN/W were investigated for five consecutive experiments. The used photocatalyst was separated from the solution, rinsed with DI water for 3 times and dried at 60°C for the next cycle.

### Scavenging experiments

The scavenging experiments were tested under 1 mM of ascorbic acid (AA), sodium oxalate (SO) and isopropanol (IPA) as the scavengers for the quenching of  $\cdot\text{O}_2^-$ ,  $\text{h}^+$  and  $\cdot\text{OH}$ . And the inhibition rates of various scavengers for the degradation of TC could be calculated by the following equations:

$$R_{\cdot\text{O}_2^-} = \frac{k_{\cdot\text{O}_2^-}}{k} = \frac{k - k_{AA}}{k} \quad (1)$$

$$R_{\text{h}^+} = \frac{k_{\text{h}^+}}{k} = \frac{k - k_{SO}}{k} \quad (2)$$

$$R_{\cdot\text{OH}} = \frac{k_{\cdot\text{OH}}}{k} = \frac{k - k_{IPA}}{k} \quad (3)$$

where  $k$  is the kinetic constants for the degradation of TC without scavengers,  $k_{\cdot\text{O}_2^-}$ ,  $k_{\text{h}^+}$  and  $k_{\cdot\text{OH}}$  is the kinetic constants of different scavengers.

### Characterization

The X-ray diffraction (XRD) spectra were carried out in Ultima IV 2036E102 (Rigaku Corporation, Japan) under Cu-K $\alpha$  radiation and the scan rate was 10°/min. Fourier transform infrared (FT-IR) spectra were tested by NICOLET iS 50 (Bruker, German) using the standard KBr disk method. The surface morphology was investigated via transmission electron microscopy (TEM, JEM-2100F). X-ray photoelectron spectroscopy (XPS, Thermo Scientific K-alpha+) was used to detect the chemical states of the elements. Electron spin resonance (ESR) was carried out by

JES-FA200 spectrometer at room temperature. Brunauer-Emmet-Teller (BET) surface areas were obtained by a nitrogen adsorption-desorption method (Micromeritics, 3Flex). UV-Vis diffuse reflectance spectra (UV-vis DRS) were characterized with a spectrophotometer (PerkinElmer, Lambda1050) in the range of 200-800 nm and using BaSO<sub>4</sub> as the reflectance standard. Photoluminescence (PL) spectra were recorded by an Edinburgh FL/FS900 spectrophotometer with an excitation wavelength of 320 nm. The photoelectrochemical (PEC) measurements were measured using a conventional three-electrode system with Na<sub>2</sub>SO<sub>4</sub> (0.1 M) as electrolyte on an electrochemical workstation (CHI6600E, CHENHUA Instrument Company). The working electrode was prepared by loading 10 mg of different catalysts onto carbon cloth (1.0 cm<sup>2</sup>). EIS were measured with an amplitude of 5 mV over a frequency range of 100 kHz to 1 Hz. Linear sweep voltammetry (LSV) curves were recorded in the voltage range at -1.0-1.0 V. The electron spin resonance (ESR) was carried out on a JES-FA200 spectrometer under visible light irradiation ( $\lambda > 420$  nm) with 5,5-dimethyl-1-pyrroline N-oxide (DMPO) in methanol and deionized water as the spin-trapping agent.

## Section 2. Supporting Figures and Tables

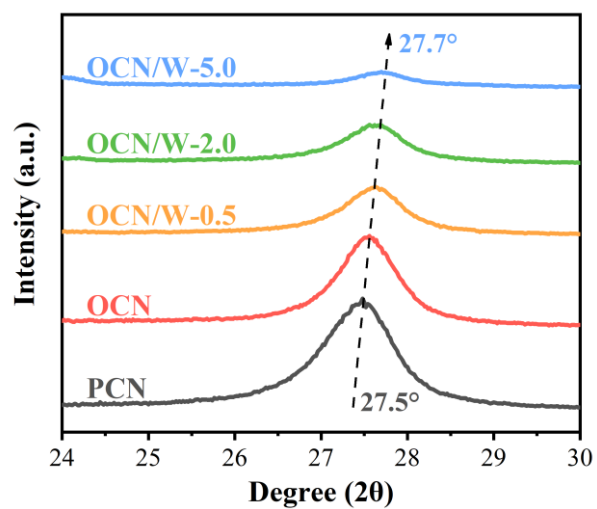


**Fig. S1** High-resolution spectra of XRD around (002) peak of the as-prepared samples

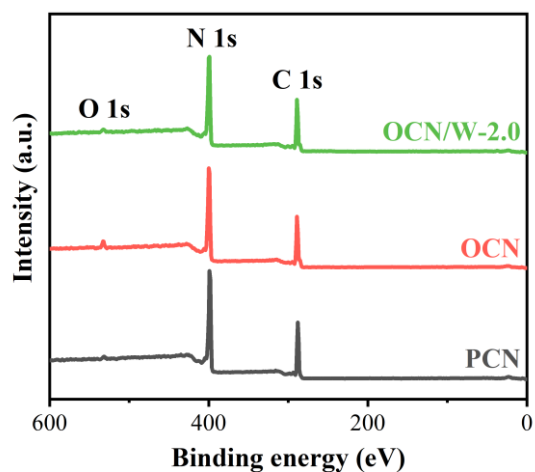


**Fig. S2** XPS survey spectra of PCN, OCN and OCN/W.

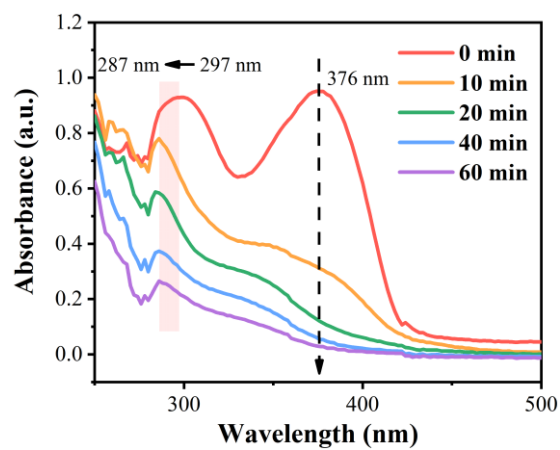


**Fig. S3** UV-Vis spectroscopy of TC degradation at different time

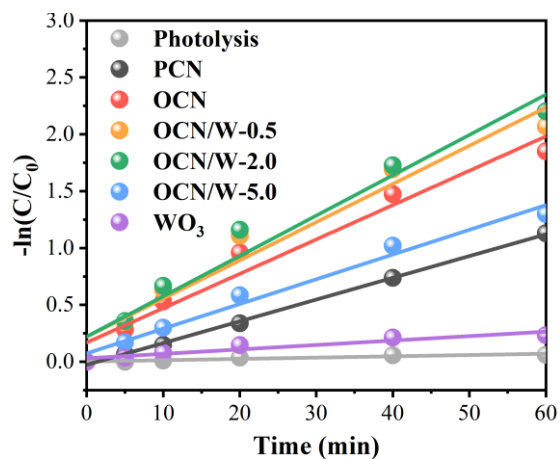


**Fig. S4** Pseudo-first-order kinetic curves of the as-prepared composites toward TC degradation under visible light irradiation

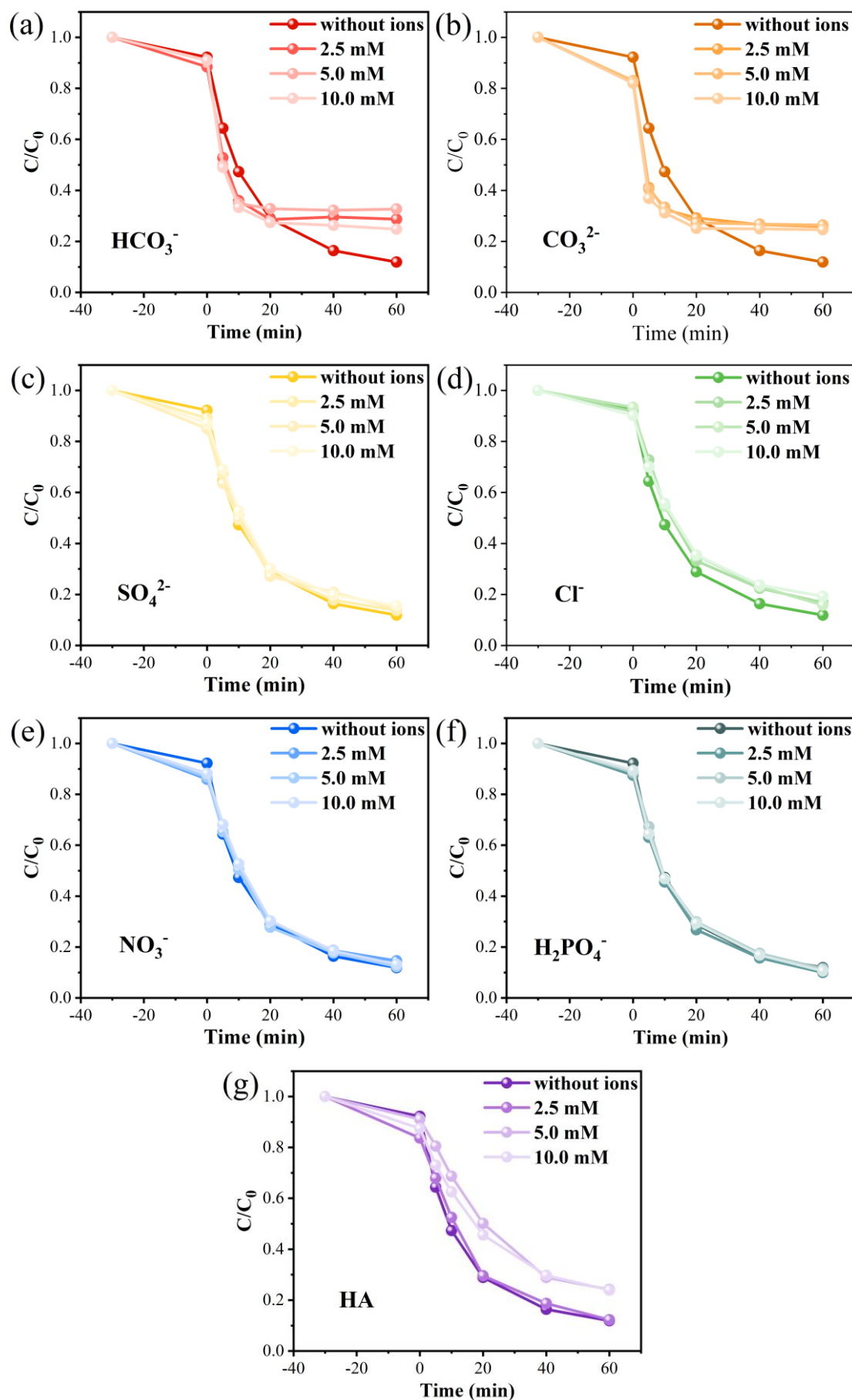


**Fig. S5** Photo-degradation of TC by OCN/W-2.0 under different concentration of (a)  $\text{HCO}_3^-$ ; (b)  $\text{CO}_3^{2-}$ , (c)  $\text{SO}_4^{2-}$ ; (d)  $\text{Cl}^-$ , (e)  $\text{NO}_3^-$ , (f)  $\text{H}_2\text{PO}_4^-$  and (g) HA.

Inorganic anions were commonly existed in natural water in the form of salts, which could have an impact on the degradation process of TC molecule by reacting with reactive radicals as shown in **Eq. (4-9)**. Herein, the effects of  $\text{HCO}_3^-$ ,  $\text{CO}_3^{2-}$ ,  $\text{SO}_4^{2-}$ ,  $\text{Cl}^-$ ,  $\text{NO}_3^-$  and  $\text{H}_2\text{PO}_4^-$  (0-10 mM) on the performance of OCN/W-2.0 were investigated. As shown in **Fig. S5a,b**, there was a double effect on the degradation of TC in the presence of  $\text{HCO}_3^-/\text{CO}_3^{2-}$ , which showed a positive effect in the early stage of reaction and a negative one in the late stage. At the initial stage of the reaction,  $\text{HCO}_3^-/\text{CO}_3^{2-}$  could improve the degradation efficiency of the reaction; however, the degradation of TC was gradually inhibited and tended to equilibrium with the progress of the reaction. On the one hand, the reaction solution was weakly alkaline as  $\text{HCO}_3^-/\text{CO}_3^{2-}$  is a weak acid which could change the existing form of TC and affect the degradation process. Studies have shown that TC is unstable under alkaline conditions and thus the photocatalytic degradation of TC is more likely to occur under this condition (Yue et al., 2015). In addition, the content of  $\cdot\text{OH}$  in the reaction system will rise under alkaline conditions, thus increasing the yield of  $\cdot\text{OH}$  in the reaction system and further promoting the photocatalytic reaction as indicated by **Eq. (6)**. On the other hand,  $\text{HCO}_3^-/\text{CO}_3^{2-}$  was proved to be an effective scavenger of  $\cdot\text{OH}$  and thus produce  $\cdot\text{CO}_3^-$  which is less reactive than  $\cdot\text{OH}$  (**Eq. (5-6)**) (Ao et al., 2019, Santiago et al., 2014, Chen et al., 2020). Based on the above analysis, the effect of  $\text{HCO}_3^-$  on the photodegradation of TC is the results of interaction between the scavenge of  $\cdot\text{OH}$  and generation of  $\cdot\text{CO}_3^-$ . The slight decrease with the existence of  $\text{SO}_4^{2-}$  could be attributed to the capture of holes by  $\text{SO}_4^{2-}$  as depicted in **Fig. S5c**. No obvious effect of  $\text{Cl}^-$ ,  $\text{NO}_3^-$  and  $\text{H}_2\text{PO}_4^-$  was observed even with the anion concentration up to 10 mM (**Fig. S5d,f**).

Besides, humic acid (HA) is a kind of organic matter that widely existing in natural water bodies including surface water and treatment plant water with the range of 0.1 mg/L to 10 mg/L (Guo et al., 2020, Ao et al., 2019). Therefore, the influence of HA on the TC degradation was also evaluated (**Fig. S5g**). The photocatalytic activity was decreased with the increase of HA concentration. The removal rate of TC was decreased by 12% in the presence of 10 mg/L HA compared with the control experiment, and it decreased with the increase of HA concentration. The inhibition of HA toward TC degradation could be corresponded to the competition of reactive species or photons between HA and TC or OCN/W-2.0 (Guo et al., 2020, Song et al., 2017). However, the degradation rate of TC was still reach to 76.1% even the HA concentration was 10 mg/L. The above results implying that OCN/W-2.0 is able to resist the negative effects of those anions and HA and has the potential in practical applications due to the introduction of O atom and the formation of

Z-scheme heterojunction with WO<sub>3</sub>.

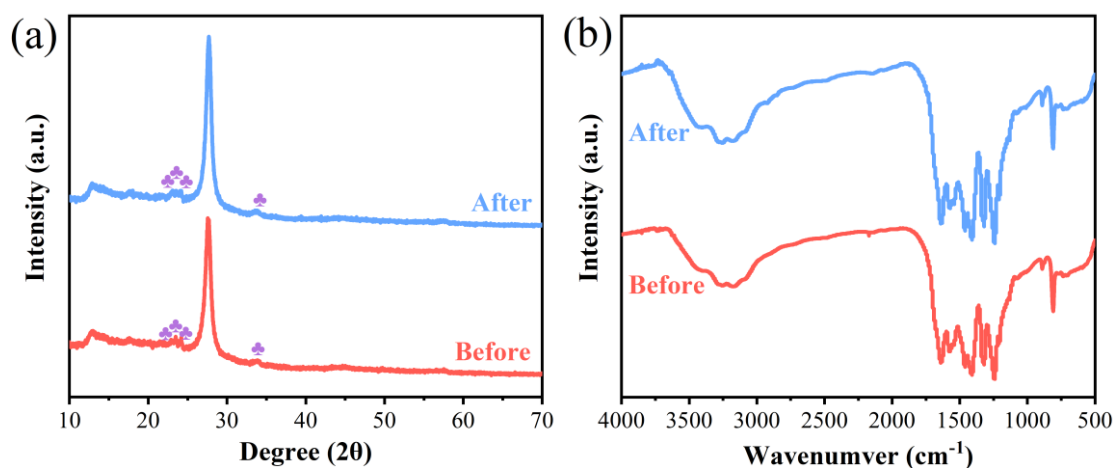


**Fig. S6** The (a) XRD and (b) FTIR spectra of fresh and used OCN/W-2.0 composites.

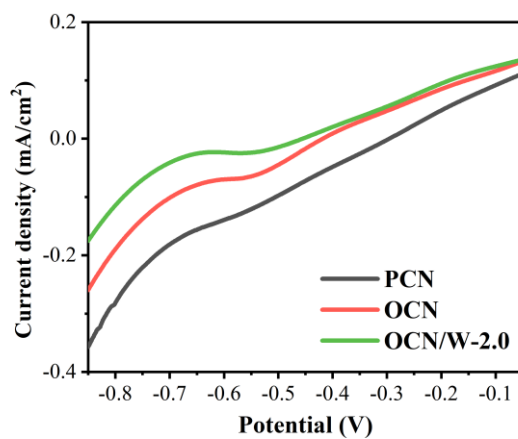


**Fig. S7** LSV curves of PCN, OCN and OCN/W-2.0 composites.

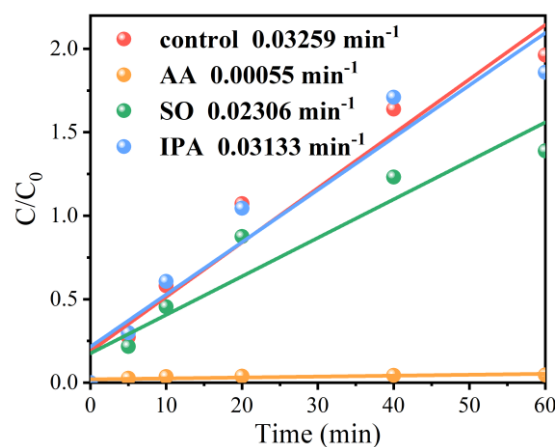


**Fig. S8** Pseudo-first-order of the photocatalytic degradation of TC under visible light irradiation with different scavengers.

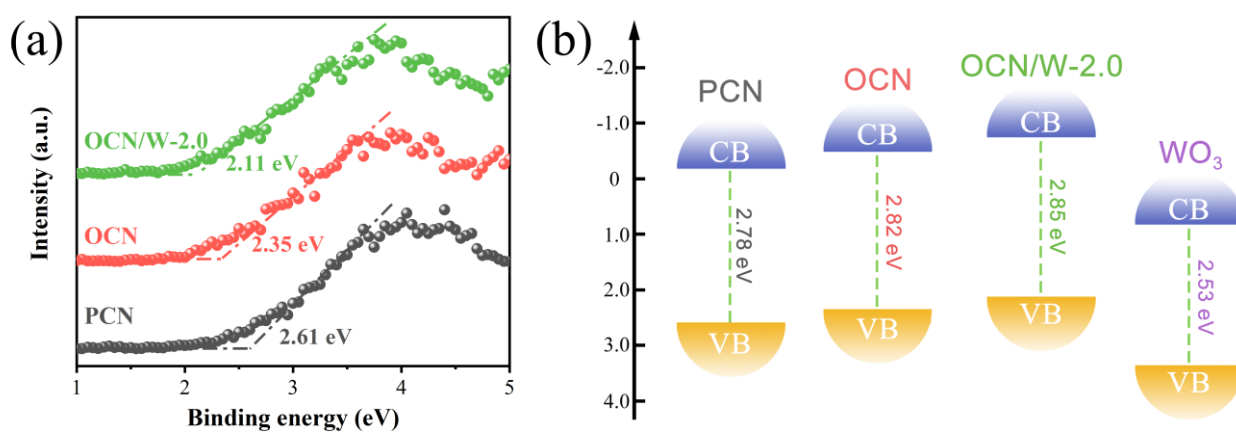


**Fig. S9** (a) VB-XPS spectra of PCN, OCN and OCN/W-2.0; (b) band structure of PCN, OCN, OCN/W-2.0 and  $\text{WO}_3$ .

**Table S1** Atom concentration for C, N and O elements derived from the XPS spectra

Sample	C/at.%	N/at.%	O/at.%	W/at.%	C/N atomic ratio
PCN	38.97	59.78	1.25	/	0.65
OCN	40.68	56.37	2.95	/	0.72
OCN/W	40.72	57.69	1.50	0.08	0.70

**Table S2** XPS N 1s spectra results of PCN, OCN and OCN/W

Sample	N <sub>2c</sub>	N <sub>3c</sub>	NH <sub>x</sub>	N <sub>2c</sub> /N <sub>3c</sub>
PCN	59.4	34.1	6.5	1.74
OCN	46.6	43.3	10.1	1.08
OCN/W	50.9	39.9	9.2	1.28

**Table S3** BET surface areas and pore volumes of different samples

Samples	Surface area (m <sup>2</sup> /g)	Pore volume (cm <sup>3</sup> /g)
PCN	9.0852	0.059021
OCN	54.5474	0.196813
OCN/W-2.0	92.2245	0.414287

**Table S4.** Comparison of photodegradation efficiency toward different pollutants of OCN/W-2.0 with other reported catalysts.

Pollutant	Catalyst	Dosage (g/L)	Pollutant concentration (mg/L)	Light source	Degradation efficiency (%)	Reaction time (min)
TC	g-C <sub>3</sub> N <sub>4</sub> -WO <sub>3</sub> (Jing et al., 2021)	0.4	10	500 W (simulated sunlight)	79.8	180
	Ag-g-C <sub>3</sub> N <sub>4</sub> -WO <sub>3</sub> (Chen et al., 2019)	0.33	10	500 W (visible light)	ca.91	140
	OCN(Guo et al., 2020)	1.0	20	300 W (visible light)	85.76	120
	g-C <sub>3</sub> N <sub>4</sub> -WO <sub>3</sub> (Yan et al., 2019)	1.0	10	300 W (visible light)	97	120
	<b>OCN/W</b>	<b>1.0</b>	<b>15</b>	<b>300 W (visible light)</b>	<b>93.9</b>	<b>60</b>
CIP	g-C <sub>3</sub> N <sub>4</sub> -WO <sub>3</sub> (Navarro-Aguilar et al., 2019)	1.0	10	35 W (simulated sunlight)	ca.90	180
	g-C <sub>3</sub> N <sub>4</sub> -WO <sub>3</sub> -RGO(Lu et al., 2019)	0.2	20	500 W (visible light)	85	180
	<b>OCN/W</b>	<b>1.0</b>	<b>20</b>	<b>300 W (visible light)</b>	<b>85.4</b>	<b>60</b>
BPA	g-C <sub>3</sub> N <sub>4</sub> -MoS <sub>2</sub> (Liu et al., 2020)	0.5	10	500 W (visible light)	96	150
	g-C <sub>3</sub> N <sub>4</sub> /BiOBr(Jing et al., 2021)	1.0	10	- (visible light)	93.1	60
	<b>OCN/W</b>	<b>1.0</b>	<b>10</b>	<b>300 W (visible light)</b>	<b>93.6</b>	<b>60</b>
MB	g-C <sub>3</sub> N <sub>4</sub> -WO <sub>3</sub> (Singh et al., 2019)	0.5	5	125 W (visible light)	97.82	160
	g-C <sub>3</sub> N <sub>4</sub> -WO <sub>3</sub> (Huang et al., 2013)	1.0	10	300W (visible light)	97	120
	<b>OCN/W</b>	<b>1.0</b>	<b>10</b>	<b>300 W (visible light)</b>	<b>100</b>	<b>40</b>

## References:

- [1] A.I. Navarro-Aguilar, S. Obregón, D. Sanchez-Martinez, D.B. Hernández-Uresti, An efficient and stable  $\text{WO}_3/\text{g-C}_3\text{N}_4$  photocatalyst for ciprofloxacin and orange G degradation, *Journal of Photochemistry and Photobiology A: Chemistry*, 384 (2019), pp. 112010.
- [2] D.E. Santiago, J. Araña, O. González-Díaz, M.E. Alemán-Dominguez, A.C. Acosta-Dacal, C. Fernandez-Rodríguez, J. Pérez-Peña, J.M. Doña-Rodríguez, Effect of inorganic ions on the photocatalytic treatment of agro-industrial wastewaters containing imazalil, *Applied Catalysis B: Environmental*, 156-157 (2014), pp. 284-292.
- [3] F. Guo, J. Chen, J. Zhao, Z. Chen, D. Xia, Z. Zhan, Q. Wang, Z-scheme heterojunction  $\text{g-C}_3\text{N}_4/\text{PDA}/\text{BiOBr}$  with biomimetic polydopamine as electron transfer mediators for enhanced visible-light driven degradation of sulfamethoxazole, *CHEM ENG J*, 386 (2020), pp. 124014.
- [4] H. Guo, C. Niu, C. Feng, C. Liang, L. Zhang, X. Wen, Y. Yang, H. Liu, L. Li, L. Lin, Steering exciton dissociation and charge migration in green synthetic oxygen-substituted ultrathin porous graphitic carbon nitride for boosted photocatalytic reactive oxygen species generation, *CHEM ENG J*, 385 (2020), pp. 123919.
- [5] H. Jing, R. Ou, H. Yu, Y. Zhao, Y. Lu, M. Huo, H. Huo, X. Wang, Engineering of  $\text{g-C}_3\text{N}_4$  nanoparticles/ $\text{WO}_3$  hollow microspheres photocatalyst with Z-scheme heterostructure for boosting tetracycline hydrochloride degradation, *SEP PURIF TECHNOL*, 255 (2021), pp. 117646.
- [6] H. Liu, J. Liang, L. Shao, J. Du, Q. Gao, S. Fu, L. Li, M. Hu, F. Zhao, J. Zhou, Promoting charge separation in dual defect mediated Z-scheme  $\text{MoS}_2/\text{g-C}_3\text{N}_4$  photocatalysts for enhanced photocatalytic degradation activity: synergistic effect insight, *Colloids and Surfaces A: Physicochemical and Engineering Aspects*, 594 (2020), pp. 124668.
- [7] H. Yan, Z. Zhu, Y. Long, W. Li, Single-source-precursor-assisted synthesis of porous  $\text{WO}_3/\text{g-C}_3\text{N}_4$  with enhanced photocatalytic property, *Colloids and Surfaces A: Physicochemical and Engineering Aspects*, 582 (2019), pp. 123857.
- [8] J. Chen, X. Xiao, Y. Wang, Z. Ye, Ag nanoparticles decorated  $\text{WO}_3/\text{g-C}_3\text{N}_4$  2D/2D heterostructure with enhanced photocatalytic activity for organic pollutants degradation, *APPL SURF SCI*, 467-468 (2019), pp. 1000-1010.
- [9] J. Singh, A. Arora, S. Basu, Synthesis of coral like  $\text{WO}_3/\text{g-C}_3\text{N}_4$  nanocomposites for the removal of hazardous dyes under visible light, *J ALLOY COMPD*, 808 (2019), pp. 151734.
- [10] L. Huang, H. Xu, Y. Li, H. Li, X. Cheng, J. Xia, Y. Xu, G. Cai, Visible-light-induced  $\text{WO}_3/\text{g-C}_3\text{N}_4$  composites

with enhanced photocatalytic activity, Dalton transactions : an international journal of inorganic chemistry, 42 (2013), pp. 866-8616.

- [11] L. Jing, D. Wang, M. He, Y. Xu, M. Xie, Y. Song, H. Xu, H. Li, An efficient broad spectrum-driven carbon and oxygen co-doped g-C<sub>3</sub>N<sub>4</sub> for the photodegradation of endocrine disrupting: Mechanism, degradation pathway, DFT calculation and toluene selective oxidation, J HAZARD MATER, 401 (2021), pp. 123309.
- [12] L. Yue, S. Wang, G. Shan, W. Wu, L. Qiang, L. Zhu, Novel MWNTs-Bi<sub>2</sub>WO<sub>6</sub> composites with enhanced simulated solar photoactivity toward adsorbed and free tetracycline in water, Applied Catalysis B: Environmental, 176-177 (2015), pp. 11-19.
- [13] M. Chen, C. Guo, S. Hou, J. Lv, Y. Zhang, H. Zhang, J. Xu, A novel Z-scheme AgBr/P-g-C<sub>3</sub>N<sub>4</sub> heterojunction photocatalyst: Excellent photocatalytic performance and photocatalytic mechanism for ephedrine degradation, Applied Catalysis B: Environmental, 266 (2020), pp. 118614.
- [14] N. Lu, P. Wang, Y. Su, H. Yu, N. Liu, X. Quan, Construction of Z-Scheme g-C<sub>3</sub>N<sub>4</sub>/RGO/WO<sub>3</sub> with in situ photoreduced graphene oxide as electron mediator for efficient photocatalytic degradation of ciprofloxacin, CHEMOSPHERE, 215 (2019), pp. 444-453.
- [15] X. Ao, W. Sun, S. Li, C. Yang, C. Li, Z. Lu, Degradation of tetracycline by medium pressure UV-activated peroxymonosulfate process: Influencing factors, degradation pathways, and toxicity evaluation, CHEM ENG J, 361 (2019), pp. 1053-1062.
- [16] Y. Song, J. Tian, S. Gao, P. Shao, J. Qi, F. Cui, Photodegradation of sulfonamides by g-C<sub>3</sub>N<sub>4</sub> under visible light irradiation: Effectiveness, mechanism and pathways, Applied Catalysis B: Environmental, 210 (2017), pp. 88-96.